CRISP1 as a novel CatSper regulator that modulates sperm motility and orientation during fertilization

Juan I. Ernesto,[1]* Mariana Weigel Muñoz,[1]* María A. Battistone,[1] Gustavo Vasen,[1] Pablo Martínez-López,[2] Gerardo Orta,[2] Dulce Figueiras-Fierro,[2] José L. De la Vega-Beltran,[2] Ignacio A. Moreno,[3] Héctor A. Guidobaldi,[4] Laura Giojalas,[4] Alberto Darszon,[2] Débora J. Cohen,[1] and Patricia S. Cuasnicú[1]

[1]Instituto de Biología y Medicina Experimental, Consejo Nacional de Investigaciones Científicas y Técnicas, C1428ADN Buenos Aires, Argentina
[2]Departamento de Genética del Desarrollo y Fisiología Molecular, Instituto de Biotecnología, Universidad Nacional Autónoma de México, Morelos 62250, México
[3]Fertility Patagonia, 8400 San Carlos de Bariloche, Argentina
[4]Centro de Biología Celular y Molecular, Instituto de Investigaciones Biológicas y Tecnológicas, Universidad Nacional de Córdoba, X5016GCA Córdoba, Argentina

Ca^{2+}-dependent mechanisms are critical for successful completion of fertilization. Here, we demonstrate that CRISP1, a sperm protein involved in mammalian fertilization, is also present in the female gamete and capable of modulating key sperm Ca^{2+} channels. Specifically, we show that CRISP1 is expressed by the cumulus cells that surround the egg and that fertilization of cumulus–oocyte complexes from CRISP1 knockout females is impaired because of a failure of sperm to penetrate the cumulus. We provide evidence that CRISP1 stimulates sperm orientation by modulating sperm hyperactivation, a vigorous motility required for penetration of the egg vestments. Moreover, patch clamping of sperm revealed that CRISP1 has the ability to regulate CatSper, the principal sperm Ca^{2+} channel involved in hyperactivation and essential for fertility. Given the critical role of Ca^{2+} for sperm motility, we propose a novel CRISP1-mediated fine-tuning mechanism to regulate sperm hyperactivation and orientation for successful penetration of the cumulus during fertilization.

Introduction

Fertilization is a complex process involving a series of orchestrated steps. Spermatozoa leaving the testis must first undergo the physiological changes of maturation in the epididymis and then capacitation in the female tract (Yanagimachi, 1994). As a consequence, sperm become able to undergo the acrosome reaction (AR), an exocytotic event that takes place in the head, and to develop a vigorous and intermittent flagellar movement termed hyperactivation. These two capacitation-associated events will allow sperm to pass through the cumulus oophorus that surround the egg, to bind to and penetrate the zona pellucida (ZP), and, finally, to fuse with the egg plasma membrane. The mechanisms underlying these processes still remain to be fully elucidated but one molecule that appears to be involved is epididymal protein CRISP1, the first identified member of the highly evolutionarily conserved cysteine-rich secretory protein (CRISP) family. CRISP members (molecular mass of 20–30 kD) are characterized by the presence of 16 conserved cysteines, 10 of which are located in the C-terminal region containing both a cysteine-rich domain (CRD) and a hinge that connects the CRD to the plant pathogenesis-related 1 domain located in the N terminus (Guo et al., 2005; Gibbs et al., 2008). Evidence suggests that CRISP proteins have evolved to perform a variety of functions that rely on these different domains (Guo et al., 2005). In mammals, four CRISP proteins have been described (CRISP1–4), which are mainly expressed in the male reproductive tract and, to a lesser extent, in other tissues (Gibbs et al., 2008).

CRISP1, first described by our group (Cameo and Blaquier, 1976), is secreted by the epididymal epithelium in an androgen-dependent manner and associates with the sperm surface during epididymal transit (Kohane et al., 1980; Cohen et al., 2000b). Two populations of CRISP1 have been detected in sperm: one loosely associated and another one strongly bound to the cells, which behaves as an integral membrane protein. The loosely associated CRISP1 is released during capacitation and has been proposed as a decapacitation factor (Kohane et al., 1980; Cohen et al., 2000b; Roberts et al., 2003). In contrast, the strongly bound protein remains in sperm even after the AR (Rochwerger and Cuasnicu, 1992; Cohen et al., 2000b), and has been reported to be involved in both binding to the ZP and gamete fusion through its interaction with egg-complementary sites (Rochwerger et al., 1992; Cohen et al., 2000a; Busso et al., 2007). Experiments using a mouse line deficient for CRISP1 that constituted the first knockout for a CRISP family member revealed that, although fertile, the mutant mice have sperm with

*J.I. Ernesto and M. Weigel Muñoz contributed equally to this paper.

Correspondence to Patricia S. Cuasnicú: pcuasnicu@ibyme.conicet.gov.ar or pcuasnicu@gmail.com

Abbreviations used in this paper: AR, acrosome reaction; CASA, computer assisted sperm analysis; COC, cumulus oocyte complexes; CRD, cysteine-rich domain; CRISP, cysteine-rich secretory protein; E_m, membrane potential; I-V, current-voltage; ZP, zona pellucida.

The Rockefeller University Press $30.00
J. Cell Biol. Vol. 210 No. 7 1213–1224
www.jcb.org/cgi/doi/10.1083/jcb.201412041

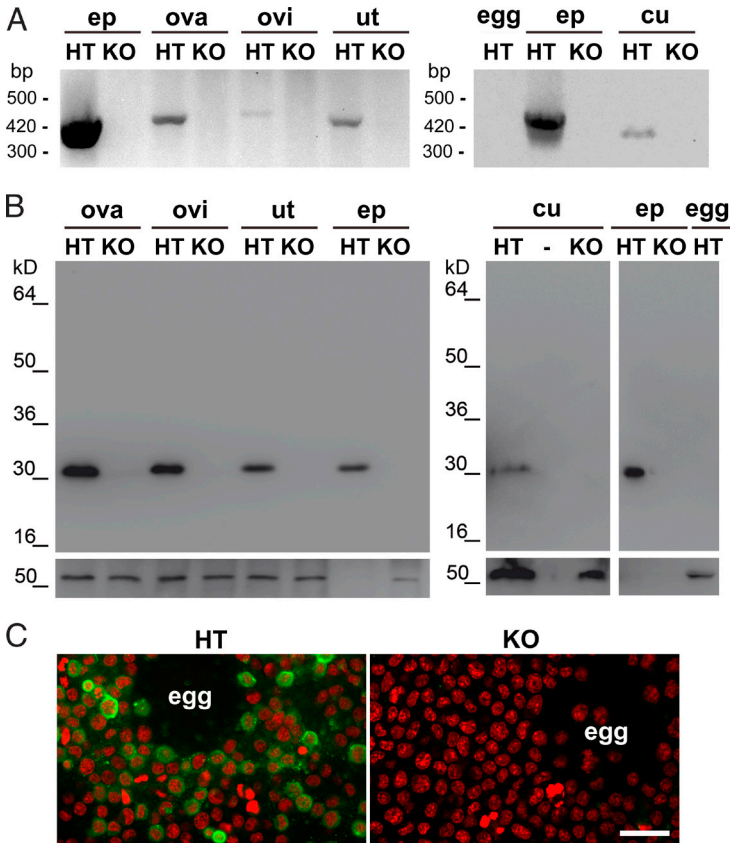

Figure 1. **CRISP1 expression in the female tract.** (A) Total RNA from ovary (ova), oviduct (ovi), uterus (ut), cumulus cells (cu), and eggs (egg) of *Crisp1*$^{+/-}$ (HT) or *Crisp1*$^{-/-}$ (KO) mice was subjected to RT-PCR using specific primers for CRISP1. In both cases epididymis (ep) was used as control. Products were separated on 2% agarose gels and stained with ethidium bromide for visualization. (B) Protein extracts (100 µg) obtained from ovary, oviduct, and uterus (left) and from cumulus cells and eggs (right) as well as from the epididymis (0.2 µg; used as control) from *Crisp1*$^{+/-}$ or *Crisp1*$^{-/-}$ mice were subjected to SDS-PAGE and Western blotting using anti-CRISP1 (top) or anti-tubulin (bottom) as primary antibodies. (C) COC from *Crisp1*$^{+/-}$ and *Crisp1*$^{-/-}$ animals were washed, fixed, and subjected to indirect immunofluorescence using anti-CRISP1 as primary antibody (green). DNA staining with propidium iodide is shown in red. Bar, 30 µm.

an impaired ability to fertilize both zona-intact and zona-free eggs (Da Ros et al., 2008), confirming the proposed roles for the protein in fertilization. Moreover, the functional roles of CRI SP1 can be extended to the human homologue protein as indicated by our studies supporting the involvement of human CRI SP1 in both sperm–ZP interaction and gamete fusion (Cohen et al., 2001; Maldera et al., 2014).

Whereas the role of CRISP1 expressed in the male tract has been studied extensively, only scattered information is available on the presence of this protein in the mammalian female tract (Reddy et al., 2008; Burnett et al., 2012). In this regard, it is known that allurin, a nonmammalian homologue of CRISP proteins, is secreted in the oviduct of the frogs *Xenopus leavis* and *Xenopus tropicalis* (Olson et al., 2001; Burnett et al., 2008), binds to their egg jelly, and exerts a chemoattractant effect in vitro not only on frog but also on mouse sperm (Xiang et al., 2005; Burnett et al., 2011a). The presence of a CRISP homologue (~60% homology with CRISP1) in the nonmammalian female tract with a function in fertilization opened the possibility that CRISP1 expressed in the mammalian female tract could also play a role in gamete interaction. In the present work, we provide evidence supporting that CRISP1 is expressed by the cumulus cells and plays a role in fertilization by modulating sperm orientation, hyperactivation, and key Ca^{2+} channels in sperm.

Results

CRISP1 is expressed in the female tract and participates in cumulus penetration

As a first step toward the evaluation of CRISP1 expression in the female tract, the presence of mRNA for *Crisp1* was analyzed by RT-PCR in the ovaries, oviducts, and uteri as well as in the eggs and cumulus cells from *Crisp1*$^{+/-}$ and *Crisp1*$^{-/-}$ females using mouse epididymal mRNA as a positive control. As shown in Fig. 1 A, a band of the expected size for *Crisp1* was observed in the three female tissues tested and cumulus cells but not in the egg. In all the cases, the identity of the amplified fragments was confirmed by DNA sequencing. The presence of CRISP1 protein along the female tract was analyzed in *Crisp1*$^{+/-}$ and *Crisp1*$^{-/-}$ tissues by Western blotting using a specific antibody against the protein. A band with a molecular mass corresponding to that of epididymal CRISP1 was observed in ovary, oviduct, uterus, and cumulus cells, although with a clearly lower intensity than that of the control epididymal protein extracts (Fig. 1 B). Indirect immunofluorescence studies revealed the presence of labeling in cumulus cells from control *Crisp1*$^{+/-}$ mice and their absence in the *Crisp1*$^{-/-}$ samples (Fig. 1 C).

The finding that CRISP1 was present in the cumulus cells led us to evaluate its involvement in the fertilization process. For this purpose, *Crisp1*$^{+/-}$ and *Crisp1*$^{-/-}$ cumulus oocyte complexes (COC) were inseminated with *Crisp1*$^{+/-}$ or *Crisp1*$^{-/-}$ sperm, and the percentage of fertilized eggs was determined after 3 h of gamete coincubation. Fertilization rates were significantly lower for *Crisp1*$^{-/-}$ than for *Crisp1*$^{+/-}$ COC, supporting a role for cumulus CRISP1 in fertilization (Fig. 2 A). Moreover, whereas the fertilizing ability of *Crisp1*$^{-/-}$ sperm did not differ from that of *Crisp1*$^{+/-}$ sperm when exposed to *Crisp1*$^{+/-}$ COC, it was significantly lower than that of *Crisp1*$^{+/-}$ sperm when coincubated with COC from *Crisp1*$^{-/-}$ females (Fig. 2 A), revealing functional defects in *Crisp1*$^{-/-}$ sperm not detectable when using control COC. To further characterize the role of cumulus CRISP1 during fertil-

ization, *Crisp1*$^{+/-}$ and *Crisp1*$^{-/-}$ COC were inseminated with Hoechst-stained capacitated sperm of both genotypes and the number of bright sperm heads within each cumulus was determined 15 min after gamete coincubation. Results revealed a significantly lower number of sperm within *Crisp1*$^{-/-}$ COC than within control *Crisp1*$^{+/-}$ COC regardless of the sperm *Crisp1* genotype (Fig. 2 B), supporting the relevance of cumulus CRISP1 for cumulus penetration. One possible explanation for this observation is that the absence of CRISP1 affects the structure and/or organization of the cumulus matrix, making it less penetrable. To evaluate this possibility, we examined the spontaneous as well as the hyaluronidase-induced dispersion of *Crisp1*$^{+/-}$ and *Crisp1*$^{-/-}$ COC as a function of time. Although a time-dependent decrease in cumulus integrity was observed in both the spontaneous and hyaluronidase-induced COC dispersion assays, no significant differences between *Crisp1*$^{+/-}$ and *Crisp1*$^{-/-}$ COC were detected (Fig. S1). To analyze whether the decrease in COC penetration could be attributed to an effect of the protein on the AR, cumulus penetration assays were performed using green/red fluorescent sperm, which allow the detection of their acrosomal status (Hasuwa et al., 2010). Although the number of penetrating sperm was lower in *Crisp1*$^{-/-}$ COC than in controls (10.3 ± 2.2 sperm/*Crisp1*$^{-/-}$ vs. 14.7 ± 2.9 sperm/*Crisp1*$^{+/-}$, $n = 5$, $P < 0.05$), the percentage of acrosome-reacted sperm within the COC was similar regardless of the female *Crisp1* genotype (51 ± 12% *Crisp1*$^{-/-}$ vs. 50 ± 6% *Crisp1*$^{+/-}$, $n = 5$, NS). Moreover, when *Crisp1*$^{+/-}$ sperm were incubated under capacitating conditions in the presence of CRISP1, no differences were observed in the percentages of spontaneous and progesterone-induced AR compared with controls (Fig. S2).

CRISP1 regulates sperm orientation and hyperactivation

Based on the chemoattractant activity of allurin (Burnett et al., 2011a), the possibility that cumulus CRISP1 could be acting as a sperm guiding molecule was also explored using an assay that involves the direct microscopic observation of sperm swimming up a chemoattractant gradient in a modified Zigmond chamber (Guidobaldi et al., 2008). One well of the chamber was loaded with capacitated mouse sperm and the second well was loaded with different concentrations of purified rat CRISP1 (1 pM to 10 µM). COC-conditioned medium and progesterone (100 pM) were used as positive controls because both have been described as chemoattractants in other species (Sun et al., 2005; Teves et al., 2006; Guidobaldi et al., 2008). CRISP1 at 1 µM produced a significant increase in the percentage of oriented sperm, reaching levels not different from those corresponding to the positive controls when used at 10 µM (Fig. 3 A). Subsequent structure/function studies revealed that protein conformation is relevant for CRISP1 sperm-orienting activity as judged by the finding that heat-denatured and DTT-treated native CRISP1 as well as bacterially expressed recombinant CRISP1 showed no effect on the percentage of oriented sperm (Fig. 3 A). Considering that sperm are likely already hyperactivated at the moment of reaching the egg, and that hyperactivation requires modulation to direct sperm toward the egg (Chang and Suarez, 2010, 2011; Armon and Eisenbach, 2011; Boryshpolets et al., 2015), motility patterns (i.e., hyperactivated, transitional, and linear) were analyzed in those sperm exposed to either a CRISP1 gradient or control media in the chamber. CRISP1 treatment produced a significant decrease in the percentage of hyperactivation with no changes in the proportion of cells with linear pattern compared with controls (Fig. 3 B, top; and Fig. S3). Furthermore, the CRISP1-oriented population exhibited significantly lower percentages of hyperactivated cells accompanied by significantly higher levels of sperm with linear pattern compared with nonoriented cells (Fig. 3 B, bottom). Together, these observations support the idea that the orienting properties of CRISP1 are linked to the ability of the protein to regulate sperm hyperactivation. This ability was confirmed by computer assisted sperm analysis (CASA) studies showing that exposure of capacitated sperm to native CRISP1 produced a significant reduction in different motility parameters associated with hyperactivation as well as in the percentage of hyperactivated cells (Table S1).

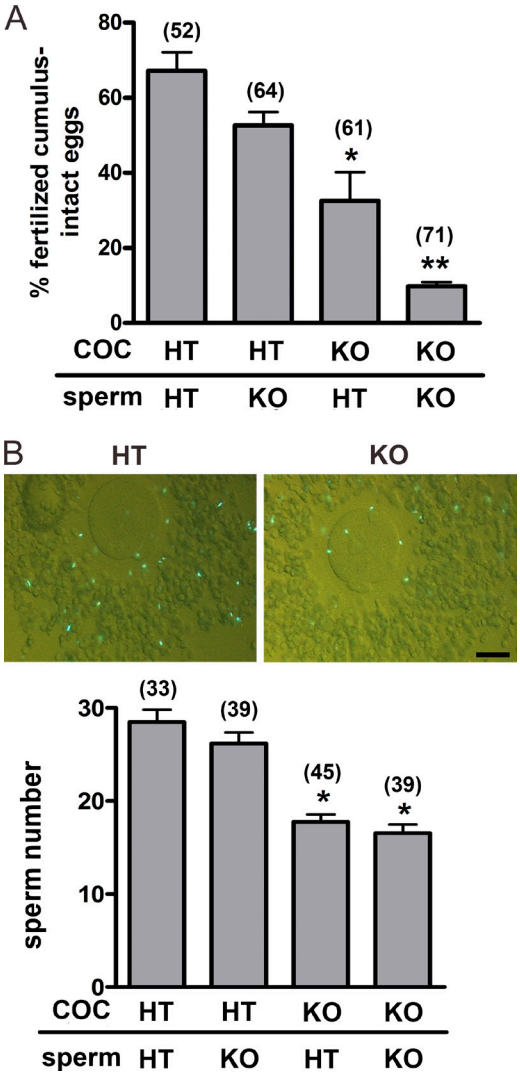

Figure 2. **Participation of cumulus CRISP1 in fertilization.** (A) COC from *Crisp*$^{+/-}$ (HT) and *Crisp1*$^{-/-}$ (KO) mice were coincubated with capacitated *Crisp1*$^{+/-}$ or *Crisp1*$^{-/-}$ sperm for 3 h and then stained with Hoechst 33342 for evaluation of fertilization. Results represent the mean ± SEM of three independent experiments. *, $P < 0.05$ vs. *Crisp1*$^{+/-}$ COC; **, $P < 0.001$ vs. all groups. (B) *Crisp1*$^{+/-}$ and *Crisp1*$^{-/-}$ COC were coincubated for 15 min with capacitated *Crisp1*$^{+/-}$ or *Crisp1*$^{-/-}$ sperm previously loaded with Hoechst 33342, and the number of sperm observed within the cumulus (top) was determined (bottom). Results represent the mean ± SEM of five independent experiments. *, $P < 0.05$ vs. *Crisp1*$^{+/-}$ COC. The total numbers of eggs analyzed in each case are indicated in parentheses. Bar, 50 µm.

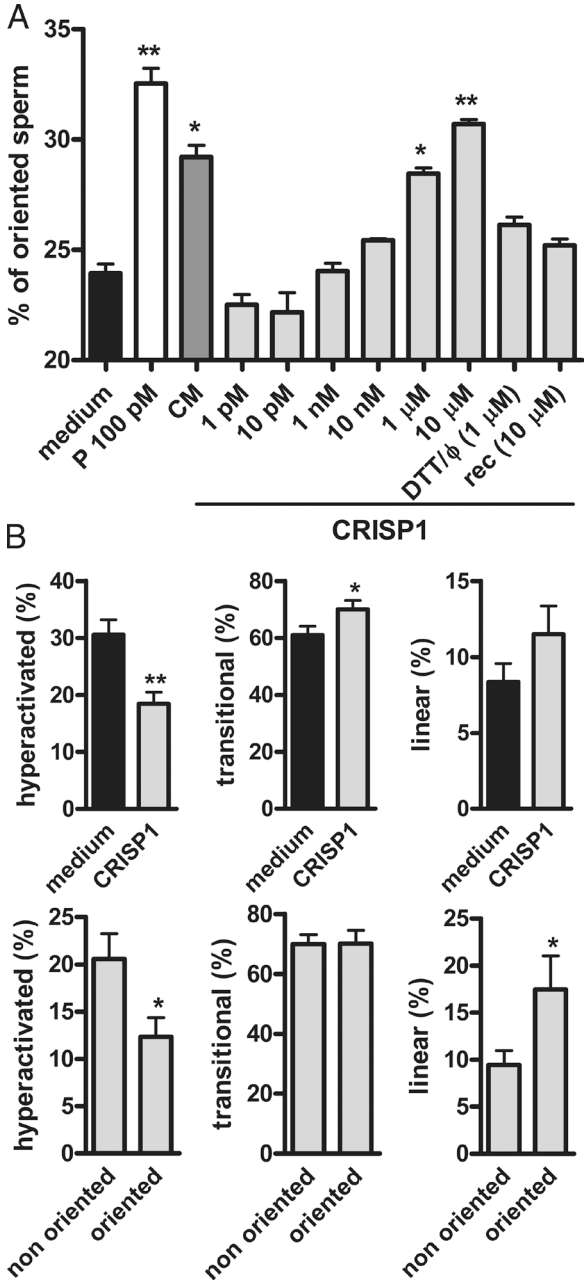

Figure 3. **Sperm orientation and motility in the presence of CRISP1.** (A) Capacitated sperm were placed in one well of a modified Zigmond chamber and CRISP1 (1 pM to 10 µM), DTT-treated and heat-denatured CRISP1 (1 µM; DTT/Φ), or recombinant CRISP1 (10 µM; rec) were loaded in the second well. Medium alone was used as negative control and both progesterone (100 pM; P) and cumulus-conditioned medium (CM) were used as positive controls. After 15 min, the percentage of oriented sperm toward the corresponding gradients was calculated by analyzing sperm trajectories. In all cases, results represent the mean ± SEM of at least three independent experiments in which >150 sperm trajectories per experiment were analyzed. *, $P < 0.05$; **, $P < 0.005$ vs. medium. (B) Percentages of hyperactivated (left), transitional (middle), or linear (right) patterns of motility for sperm exposed to either CRISP1 (1 µM) or medium (control; top) and for oriented and nonoriented cells within the CRISP1-exposed group (bottom). In all cases, results represent the mean ± SEM of seven independent experiments in which at least 100 sperm trajectories per experiment were analyzed. **, $P < 0.005$; *, $P < 0.05$.

CRISP1 inhibits mouse sperm TRPM8 and CatSper Ca^{2+} channels

Evidence shows that regulation of sperm motility, orientation, and hyperactivation makes use of intracellular Ca^{2+} signals (Publicover et al., 2008; Alasmari et al., 2013). Given the known ion channel regulatory activity of CRISP proteins (Gibbs et al., 2008, 2011), we hypothesized that CRISP1 modulates sperm hyperactivation and orientation at the molecular level through its ability to regulate Ca^{2+} channels. Considering previous findings indicating that CRISP4 inhibited TRPM8 channels in testicular sperm (Gibbs et al., 2011) and that it was not possible to electrophysiologically detect TRPM8 currents in epididymal sperm (Lishko et al., 2012; Zeng et al., 2013), we initially evaluated the effect of CRISP1 on total cationic currents evoked in testicular sperm. For this purpose, the cells were patch clamped via the cytoplasmic droplet exposed to physiological solution (HS media, with impermeable anions). CRISP1 was used at 10 µM because this was the concentration at which CRISP4 was shown to produce inhibition in TRPM8 (Gibbs et al., 2011) and CRISP1 had the highest sperm-orienting activity (this paper). Fig. 4 A shows representative currents (filtered at 2 kHz) evoked from a 0-mV holding potential by square voltage steps, lasting 350 ms, from −100 to +100 mV in 20-mV increments. At positive potentials, the currents rapidly activated and had a minor slowly activating component (Fig. 4 A, left). The addition of 10 µM CRISP1 to sperm attenuated both inward and outward currents (Fig. 4 A, right). Fig. 4 B illustrates the current-voltage (I-V) curves obtained from experiments shown in Fig. 4 A. Specifically, between +25 and +100 mV, 10 µM CRISP1 reduced the conductance, leading to a maximal inhibition of 22.0 ± 3.5% (+100 mV), whereas at −100 mV, inhibition was 37.5 ± 2.0%. No inhibition was observed in control experiments using heat-denatured CRISP1 (Fig. 4 C), indicating the specificity of the inhibition. As can be seen from the I-V curves, the CRISP1 inhibition was mildly stronger at negative potentials. To further define the inhibitory effect of CRISP1, the whole-cell currents from testicular sperm were recorded by using Cs^+ as the main current carrier, a usual experimental condition to study transient receptor potential (TRP) currents (Grimm et al., 2003). In addition, the functional presence of TRPM8 channels in testicular mouse sperm was corroborated by recording cold temperature-activated currents (Fig. S4). Cauda epididymal sperm, however, did not display temperature-activated TRPM8 currents (Fig. S4). Fig. 4 D (left) shows currents from testicular sperm activated by the indicated voltage protocol, which exhibits a small and slow inactivating component at more negative potentials. Fig. 4 (D [right] and E) also illustrates that 10 µM CRISP1 inhibited 37.5 ± 2.0% at −100 mV and 18.5 ± 5.0% at +100 mV ($n = 3$) of the current. Furthermore, currents stimulated with menthol (300 µM; 65.0 ± 15.0% at +130 mV, $n = 3$; see Fig. 4, F [left and middle] and G), a classic TRPM8 agonist (Mälkiä et al., 2007), were partially inhibited by 10 µM CRISP1 (32.2 ± 14.0% at −100 mV and 24.6 ± 11.0% at +100 mV; Fig. 4, F [right] and G). This effect can be observed in the I-V curves of the menthol- and CRISP1-sensitive current components (Fig. 4 G). In addition, the I-V curves show again that the CRISP1 effect is slightly more potent at negative potentials and that, as the reversal potential is close to zero, the main ion carrying the current is Cs^+ (see Materials and methods). Altogether, these results are consistent with the presence of functional TRPM8 channels sensitive to CRISP1 in testicular mouse sperm.

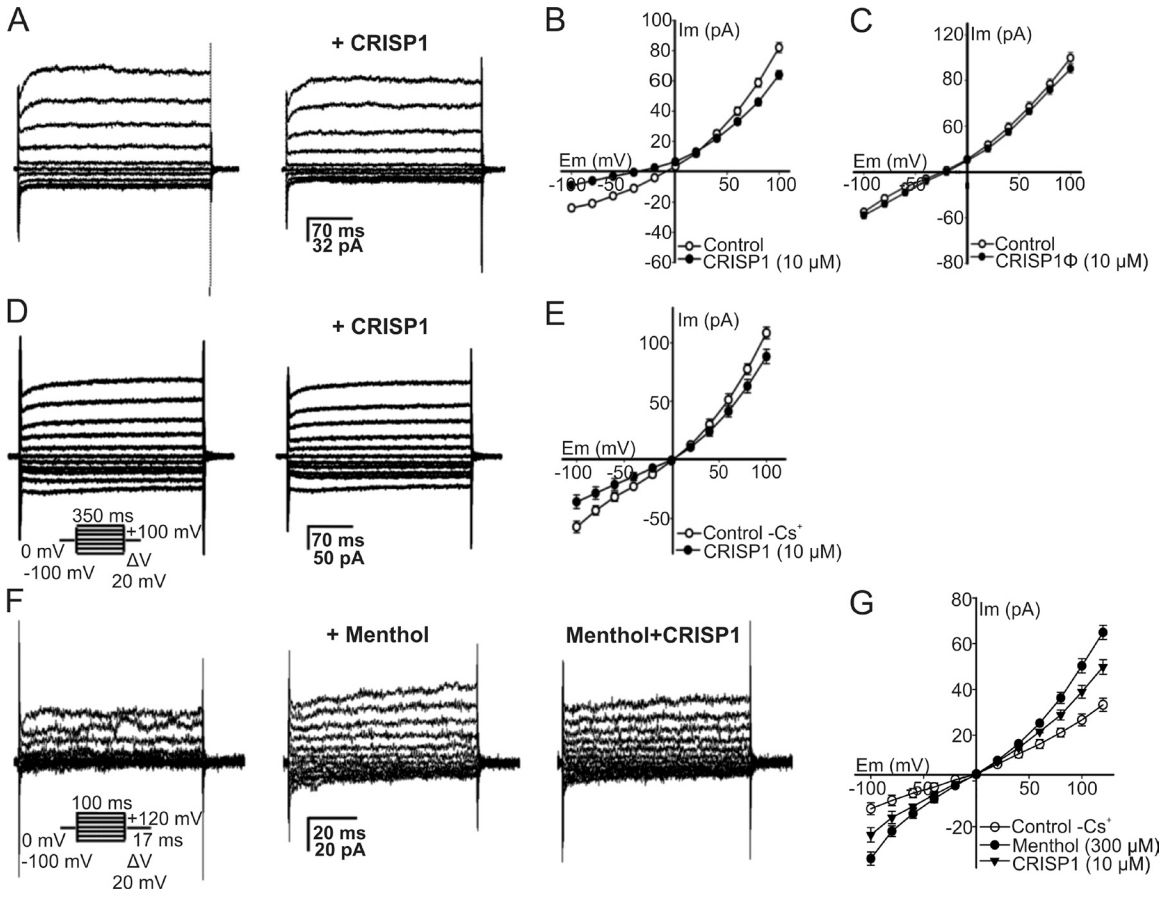

Figure 4. **CRISP1 inhibits the macroscopic cationic currents in testicular sperm.** (A) Representative whole-cell patch clamp currents recorded on a testicular sperm at the cytoplasmic droplet. The currents were evoked applying voltage steps (20 mV) from a holding potential of 0 mV to test potentials ranging from −100 to +100 mV in cationic solution (HS media with impermeable anions). The protocol used for eliciting cationic currents in A and D is shown below traces in D. Representative whole-cell currents under control conditions (left) and after adding 10 µM CRISP1 using a picospritzer close to the sperm (right). (B) Mean I-V curves from experiments as in A. Results represent the mean ± SEM of four independent experiments. (C) Mean I-V relationship of cationic currents in the presence of 10 µM of heat-denatured CRISP1 (CRISP1Φ) compared with the control. The currents were elicited with the same voltage protocol as in A. (D) Currents recorded from sperm in the Cs^+ recording solution. Representative whole-cell currents under control conditions (left) and after adding 10 µM CRISP1 (right). (E) I-V curves show inhibition by 10 µM CRISP1 of the control sperm Cs^+ currents. (F) Control Cs^+ whole-cell currents recorded with the same solutions as in D applying the voltage protocol in the inset (left) were stimulated by 300 µM menthol (middle). The stimulated current was inhibited by 10 µM CRISP1 (right). (G) Mean I-V curves from experiments as in F. Results represent the mean ± SEM of three experiments; in some cases, the SEM bars were smaller than symbols.

The fact that menthol can also activate human CatSper (Brenker et al., 2012) led us to test whether CRISP1 could inhibit this channel. As a first approximation, the membrane potential of epididymal sperm was measured with a fluorescent cyanine dye using a protocol that unveils the activity of CatSper by suddenly removing external Ca^{2+} after adding 3.5 mM EGTA. Because reducing external Ca^{2+} below 65 nM allows CatSper to efficiently conduct monovalent cations (Kirichok et al., 2006), at the resting potential of noncapacitated sperm (approximately −45 mV), it conducts Na^+, depolarizing the cells (Espinosa and Darszon, 1995; Torres-Flores et al., 2011). As anticipated, this depolarization is inhibited by 1 µM NNC 55-0396 and 500 µM Ni^{2+} used to reduce CatSper activity (Kirichok et al., 2006; Strünker et al., 2011; Alasmari et al., 2013) as well as by HC-056456 (10 µM), a compound reported to be an effective blocker of both CatSper and sperm hyperactivation (Fig. 5 A; Carlson et al., 2009). Whereas 10 µM CRISP1 significantly inhibited the depolarization caused by EGTA addition, neither the saline solution used to prepare CRISP1 nor heat-denatured CRISP1 had a significant effect (Fig. 5 A), suggesting that CRISP1 inhibits CatSper channels in mouse sperm. Furthermore, CRISP1 also inhibited 53.0 ± 4.3% (n = 3) of the menthol-induced intracellular Ca^{2+} concentration increase in single epididymal sperm imaging experiments (Fig. S5). To corroborate these results, we recorded CatSper currents from cauda epididymal sperm using a voltage-ramp protocol and Cs^+ as the main conducting ion in the absence of divalent cations. CRISP1 inhibited >50% of the CatSper currents at negative and positive potentials, whereas heat-denatured CRISP1 had no effect (Fig. 5, B and C). Altogether, these results suggest that CRISP1 is a CatSper regulatory molecule.

Discussion

CRISP1 has been considered until now to be a protein expressed in the male reproductive tract, which upon binding to sperm in the epididymis, is carried with these cells into the female tract. It has been proposed to act as a decapacitating factor (Kohane et al., 1980; Cohen et al., 2000b, 2011; Roberts

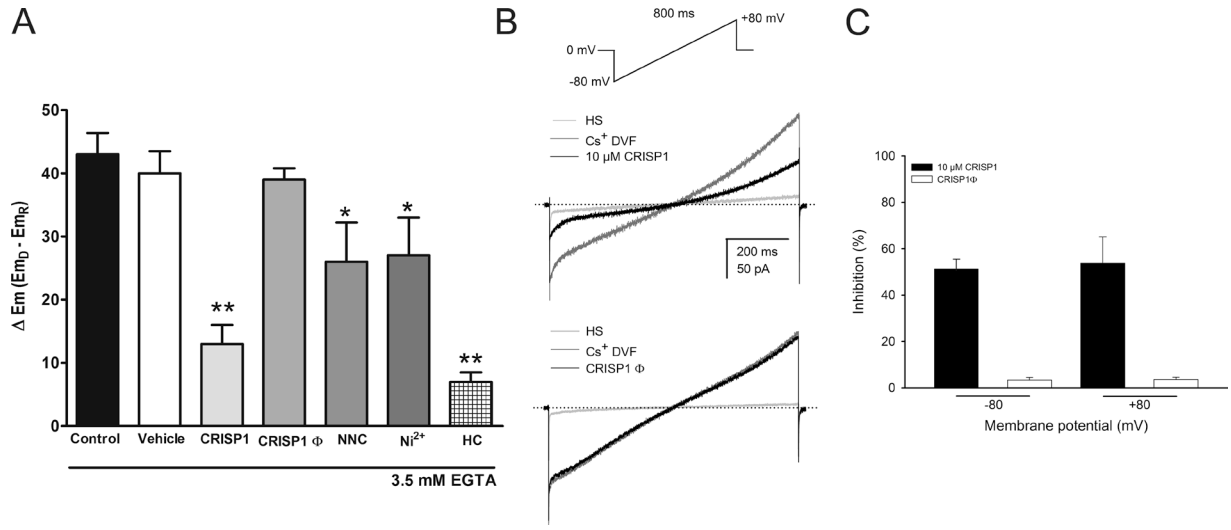

Figure 5. **CRISP1 inhibits CatSper channels in cauda epididymal sperm.** (A) CRISP1 inhibition of CatSper was evaluated measuring E_m (see Materials and methods) in Whitten's media after adding 3.5 mM EGTA, which depolarizes noncapacitated sperm caused by Na^+ influx partly through CatSper. ΔE_m represents the difference between E_m after EGTA addition (E_{mD}) and before (resting E_m [E_{mR}]) for control sperm (n = 13) or sperm incubated for 10 min with saline solution either alone (vehicle, n = 4) or containing 10 µM CRISP1 (n = 11), heat-denatured CRISP1 (CRISP1Φ; n = 6), 1 µM NNC 55-0396 (n = 7), 500 µM Ni^{2+} (n = 4), or 10 µM HC-056456 (n = 3). Results are expressed as the mean ± SEM of the number of indicated independent experiments. *, $P < 0.05$; **, $P < 0.001$ vs. control. (B) Whole-cell currents elicited by a voltage ramp from a holding potential of 0 mV (see protocol in top panel) in physiological solution (HS) or in Cs^+ divalent-free (Cs^+ DVF) medium either alone or containing CRISP1 10 µM. Note the strong inhibition effect at both negative and positive potentials (top). Under the same experimental conditions, heat denatured CRISP1 (10 µM; CRISP1Φ) had no effect along the tested voltage range (bottom). (C) CRISP1 (10 µM) inhibited ∼50% of the CatSper current at both negative and positive voltages (−80 and +80 mV) and heat-denatured CRISP1 had no effect at any voltage. Results represent mean ± SEM of five different sperm.

et al., 2003) and to be involved in modulating sperm interaction with the ZP and the egg plasma membrane (Rochwerger et al., 1992; Cohen et al., 2000a, 2001; Busso et al., 2007; Da Ros et al., 2008; Maldera et al., 2014). This paradigm, however, is unable to account for the fact that COC from CRISP1 knockout mice show impaired ability to be fertilized even with normal sperm, suggesting that there is a CRISP1-mediated step in sperm–egg interaction that had yet to be characterized. Here, we present evidence that CRISP1 is also expressed along the female reproductive tract including the cumulus cells that surround the egg and that CRISP1 from the female gamete plays an active role in fertilization by modulating sperm orientation, motility, and Ca^{2+} channels.

The decapacitating role originally proposed for CRISP1 was based on the partial release of the protein from sperm during capacitation (Kohane et al., 1980; Cohen et al., 2000b) and was later supported by results showing the ability of CRI SP1 to regulate protein tyrosine phosphorylation, AR, and sperm fertilizing ability (Roberts et al., 2003; Da Ros et al., 2008; Cohen et al., 2011). Considering that capacitation needs to be completed close to the fertilization site (Yanagimachi, 1994), it is likely that the uterine and/or oviductal CRISP1 described in this work contributes to the regulation of sperm capacitation to achieve a successful fertilization in the ampulla (Hunter and Rodriguez-Martinez, 2004).

The expression of CRISP1 by the cumulus cells opened the possibility for an additional role of the female protein in the fertilization process. The decreased fertilization in *Crisp1*$^{-/-}$ COC inseminated with either *Crisp1*$^{+/-}$ or *Crisp1*$^{-/-}$ sperm is consistent with this functional role. In addition, the absence of the protein in *Crisp1*$^{-/-}$ COC allowed us to detect the impaired fertilizing ability of *Crisp1*$^{-/-}$ sperm not evident when control COC were used (Fig. 2; Da Ros et al., 2008), indicating that cumulus CRISP1 overcomes the fertilizing deficiency of these sperm. This observation suggests that mating of *Crisp1*$^{-/-}$ males with *Crisp1*$^{-/-}$ females could lead to lower male fertility rates because of the lack of CRISP1 in the COC. Normal levels of fertility, however, were obtained (Da Ros et al., 2008), indicating the existence of beneficial and/or compensatory mechanisms operating in vivo that are not present under in vitro conditions. Considering that *Crisp1*$^{-/-}$ COC had a lower number of penetrating sperm than controls, it is likely that this explains the decreased in vitro fertilization rates. Interestingly, this decrease in the number of penetrating sperm was observed for both *Crisp1*$^{+/-}$ and *Crisp1*$^{-/-}$ sperm, supporting the idea that cumulus but not sperm CRISP1 is involved in cumulus penetration.

According to our observations, the reduction of sperm penetration in *Crisp1*$^{-/-}$ COC could not be attributed to a defective organization of the complex cumulus matrix nor to an effect on the extent of acrosomal exocytosis. In view of this, an alternative explanation for the lower number of sperm within *Crisp1*$^{-/-}$ COC is that cumulus CRISP1 has the ability to guide sperm toward the egg as reported for allurin (Burnett et al., 2011a). This possibility is supported by the finding that a CRISP1 gradient induces sperm orientation as progesterone and COC-conditioned medium. In addition, the radial distribution of cumulus cells that secrete CRISP1 might form a protein concentration gradient within the cumulus (a physiological requirement for sperm chemotaxis) as previously observed for progesterone (Teves et al., 2006; Guidobaldi et al., 2008).

Our observation showing that CRISP1 is able to orient sperm differs from previous results showing that recombinant mouse CRISP1 expressed in a eukaryotic system had no effect on mouse sperm orientation (Burnett et al., 2011a). This difference might be a result of the use of the recombinant instead of the native protein and/or the use of a conditioned medium containing unknown concentrations of the recombinant protein.

Our subsequent structure–function experiments showing that CRISP1 with a deficient disulfide bond content (Ellerman et al., 2002) was unable to stimulate sperm orientation, support the relevance of protein conformation and/or disulfide bond formation for CRISP1 sperm-orienting activity as previously reported for allurin (Burnett et al., 2011a,b). As synthetic peptides that mimic the hinge region of allurin in structure exhibit chemoattractant activity to sperm (Burnett et al., 2012), it is likely that the orienting ability of CRISP1 requires the proper conformation of the hinge region of the molecule.

Sperm are likely already hyperactivated before being exposed to the egg in vivo because the onset of hyperactivation precedes ovulation (Suárez and Osman, 1987). Although hyperactivation assists sperm to reach and fertilize the egg, it has been proposed that hyperactivated sperm require intermittent course corrections to reach the egg (Chang and Suarez, 2010, 2011; Armon and Eisenbach, 2011; Boryshpolets et al., 2015). Moreover, chemoattractant molecules have been proposed to be responsible for modulating the flagellar beating of hyperactivated sperm to redirect the cells into the chemoattractant gradient and toward the egg (Armon and Eisenbach, 2011; Burnett et al., 2011a). Armon and Eisenbach (2011) reported significantly lower hyperactivation levels in chemotactically responsive than nonresponsive human sperm exposed to a progesterone gradient and concluded that, upon sensing an increase in the chemoattractant concentration, the cells repress their hyperactivation and thus maintain their course toward the chemoattractant. Similarly, Burnett et al. (2011a) described that, in the presence of a gradient of the chemoattractant allurin, most mouse sperm trajectories were largely linear instead of circular, concluding that chemotaxis is accompanied by an overall change in sperm trajectory. In agreement with these studies, we observed a reduction in hyperactivation accompanied by an increase in linearity for CRISP1-oriented compared with nonoriented cells, indicating that these changes in motility behavior are linked to the guiding properties of CRISP1. Thus, this reduction in hyperactivated motility would not affect the overall sperm thrust required for penetration of the egg coats but would rather be beneficial for sperm function as indicated by the finding that the absence of the protein in *Crisp1*$^{-/-}$ COC leads to lower fertilization rates compared with controls. It is interesting to note that the trajectory of hyperactivated sperm also becomes straighter within the cumulus mass (Tesarík et al., 1990) probably because of the physical effects imposed by fluid viscosity and the granulosa cell bulk. However, the finding that sperm also swim straighter after being exposed to solubilized cumulus matrix supports a direct effect of cumulus intercellular matrix components on sperm apart from those caused by the physical properties (i.e., viscosity and granulose cells) of the cumulus mass (Tesarík et al., 1990).

Although the regulation of sperm motility and orientation is not well understood, it is clear that Ca^{2+} signaling plays a critical role in this process (Darszon et al., 2011; Yoshida and Yoshida, 2011). Based on this, we next analyzed the ability of CRISP1 to regulate sperm Ca^{2+} channels. Our results confirmed the activity of TRPM8 channels in testicular mouse sperm and their responsiveness to menthol (Martínez-Lopez et al., 2011), a classical agonist of TRPM8 (Mälkiä et al., 2007). It has been reported that menthol induces increases in epididymal mouse sperm intracellular Ca^{2+} concentration and AR sensitive to BCTC (a known TRPM8 blocker) and that these menthol-induced increases are significantly reduced in TRPM8 null sperm (Martínez-López et al., 2011). Although we and others (Lishko et al., 2012; Zeng et al., 2013) have been unable to electrophysiologically detect temperature-sensitive TRPM8 currents in epididymal sperm, we cannot exclude its potential involvement in the role of CRISP1 on sperm. Because menthol also stimulates human CatSper (Brenker et al., 2012), we examined whether CRISP1 could modulate this Ca^{2+} channel (Kirichok et al., 2006; Lishko and Kirichok, 2010) involved in sperm hyperactivation and essential for male fertility (Ren et al., 2001; Smith et al., 2013). Results revealed that CRISP1 inhibited membrane depolarization as well as CatSper currents recorded in mouse epididymal sperm, confirming the ability of the protein to block this sperm Ca^{2+} channel. The finding that CRISP1 inhibits Ca^{2+} channels is consistent with previous studies showing the blocking channel activity of several reptile venom (Morrissette et al., 1995; Brown et al., 1999; Yamazaki et al., 2002) and mammalian CRISP proteins (Gibbs et al., 2006, 2011). The ability of CRISP1 to regulate these channels is also consistent with the tail localization of TRPM8 (midpiece) and CatSper (principal piece; Ren et al., 2001; Martínez-López et al., 2011) as CRISP1 associates with both regions of the flagellum (Roberts et al., 2003; Maldera et al., 2011). Based on these observations, it is likely that the guiding role of CRISP1 is mediated by the ability of the protein to regulate Ca^{2+} channels. The ion channel regulatory ability of CRISP1 could be attributed to either the CRD in combination with the hinge (Gibbs et al., 2006, 2011) or both the CRD and the hinge independently (Wang et al., 2006; Zhou et al., 2008). This, together with the chemoattractant properties of the hinge region of allurin (Burnett et al., 2012), supports the idea that the orienting ability of CRISP1 could be mediated by an ion channel regulatory activity located in the hinge or in both the hinge and CRD. Moreover, as it has been proposed that the high specificity of CRISP proteins as ion channel blockers is gained by cooperation between the different domains (Suzuki et al., 2008), it is likely that the pathogenesis-related 1 domain also contributes to the ion channel regulatory activity and guiding properties of CRISP1. Finally, although the pathogenesis-related 1 domain has not been directly involved in ion channel regulation, the possibility that this domain mediates the chemoattractant role of CRISP1 cannot be excluded.

The novel finding that CRISP1 is capable of blocking CatSper is consistent with the lower levels of hyperactivation observed in cells exposed to CRISP1 as it has been reported that CatSper knockout sperm cannot hyperactivate (Ren et al., 2001). Moreover, the observation that hyperactivation is reduced in CRISP1-oriented compared with nonoriented sperm suggests that CRISP1 acts as a physiological regulator of hyperactivation and orientation through its ability to regulate CatSper. Considering that, differently from human CatSper, mouse CatSper is not activated by progesterone (Lishko et al., 2011; Strünker et al., 2011), which elicits Ca^{2+} signals even in CatSper null mice (Ren et al., 2001), it is likely that progesterone regulates mouse sperm orientation through other Ca^{2+}-mediated mechanisms. In this regard, whereas there are studies providing fundamental insights on chemotaxis of sperm from marine invertebrates, much less is known about the mechanisms underlying sperm orientation in mammals (Yoshida and Yoshida, 2011). In nonmammalian species, sperm swim in a straighter trajectory as long as the chemoattractant increases in concentration. When sperm experience a decreasing chemoattractant gradient, a high-amplitude Ca^{2+} signal is generated that produces a sharp flagellar bending that reorients the cells toward the peptide source. This

reorientation is followed by a period of straighter swimming and inhibited Ca^{2+} signals that accomplish the goal of moving the sperm up the gradient (Guerrero et al., 2010). According to our results, it is likely that a similar mechanism might be operating in mouse (Fig. 6). Given the ability of CRISP1 to inhibit Ca^{2+} channels, increasing concentrations of the protein close to or within the cumulus could prevent a high intracellular Ca^{2+} increase and allow sperm to swim straighter toward the egg. Conversely, decreasing concentrations of CRISP1 could allow a high Ca^{2+} influx and an increase in hyperactivation that could help sperm find the CRISP1-positive gradient and swim toward the egg. This is consistent with the idea that chemotactic guidance could be relevant over short distances very close to the egg whereas other guiding mechanisms (i.e., muscle contractions and rheotaxis) might be operating over long distances within the female reproductive tract (Guidobaldi et al., 2012; Miki and Clapham, 2013).

In summary, in this study we present three novel findings that indicate that CRISP1 from the female gamete plays an active role in fertilization. First, we demonstrate that CRISP1 is expressed by the cumulus cells, suggesting the presence of a CRISP1 gradient within the cumulus mass, and that the absence of this protein in the cumulus affects fertilization and cumulus penetration. Second, we show that such a gradient of CRISP1, if present in an in vitro assay, can orient sperm within the gradient by reducing hyperactivated motility and increasing linear swimming. Third, we show that CRISP1 is able to inhibit the conductivity of CatSper and TRPM8 channels. Collectively, we propose that CRISP1 expressed by the cumulus cells regulates CatSper and TRPM8 channels and, thus, an alternation between sperm hyperactivation and orientation to most efficiently bring the sperm into contact with the ZP. In this way, cumulus CRISP1 serves as a close-range regulator of sperm behavior that facilitates cumulus penetration, representing a novel fine-tuning mechanism for successful mammalian fertilization. Given the relevance of CatSper for fertility (Ren et al., 2001; Smith et al., 2013), our identification of CRISP1 as a physiological regulator of this key channel not only contributes to a better understanding of the molecular mechanisms involved in mammalian sperm–egg communication but also may help the development of new pharmacological tools for fertility regulation.

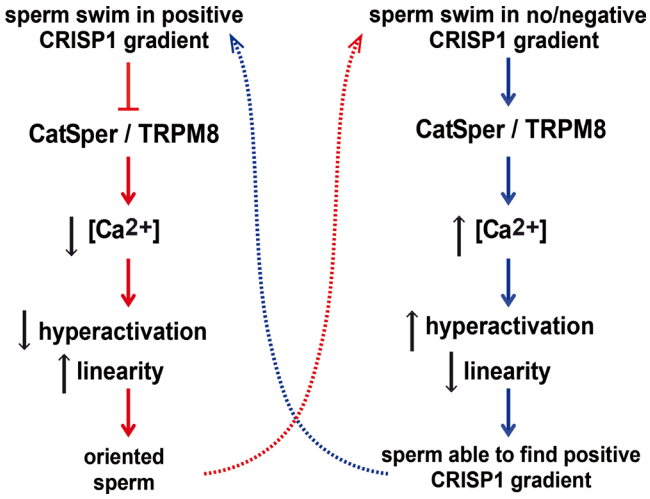

Figure 6. **Schematic model for the behavior of sperm exposed to a CRISP1 gradient.** When sperm swim along increasing CRISP1 concentrations, there is an inhibition of Ca^{2+} channels (i.e., CatSper/TRPM8) and a consequent lower entry of Ca^{2+} into the cells. This leads to lower sperm hyperactivation and higher linearity levels that maintain sperm oriented toward the positive gradient. If sperm no longer swim in increasing CRISP1 concentrations, there is no inhibition of Ca^{2+} channels and, thus, a higher Ca^{2+} influx. This results in higher hyperactivation levels that help sperm to find the positive attractant gradient again. The dotted lines indicate the dynamics of the process.

Materials and methods

Animals and reagents

Adult male (60–120 d) and young adult female (45–90 d) *Crisp1*$^{+/-}$ and *Crisp1*$^{-/-}$ (hybrid C57BL76/129SvEv-Crisp1$^{tm1Pasc/tm1Pasc}$) mice (Da Ros et al., 2008), adult CD-1 mice, and adult double-gene knockout males (BDF1-Tg [*CAG-mtDsRed2*, *Acr-EGFP*] RBGS0020sb) presenting acrosomal vesicles expressing EGFP fluorescence and midpieces (mitochondria) expressing Ds-Red2 fluorescence (Hasuwa et al., 2010; provided by M. Buffone, IBYME-CONICET, Buenos Aires, Argentina) were used. Animals were maintained at 23°C with a 12-h light/12-h dark cycle. Experiments were conducted in accordance with the Guide for Care and Use of Laboratory Animals approved by the National Institutes of Health. Procedures were approved by the Ethics Committee of Instituto de Biología y Medicina Experimenta and the local Animal Care and Bioethics Committee of Universidad Nacional Autónoma de México. All reagents and chemicals were of analytical grade and were purchased from Sigma-Aldrich or Invitrogen, unless otherwise specified. Stock solutions in DMSO were prepared for each compound and aliquots were stored at −20°C until use. In the medium, the DMSO concentration was always <0.1% and, alone, had no effect on measurement of membrane potential and channel activity.

RT-PCR analysis

Total RNA from mouse epididymis, ovary, oviduct, uterus, and cumulus cells was isolated with Trizol (Gibco) according to the manufacturer's recommendations, reverse transcribed, and subjected to PCR using primers complementary to exons 2 and 6 of the mouse *Crisp1* gene (forward, 5′-AAGCCATCAGAATTCCAAGATAGCTCTCAG-3′; and reverse, 5′-GCATGTGGAGTTGCTGAATGC-3′).

Immunoblot analysis

Epididymides, ovaries, oviducts, uteri, eggs, and cumulus cells were homogenized in lysis buffer (5 mM EDTA, 1% IGEPAL CA-630, 0.5% sodium deoxicholate, 0.1% SDS, 1% Triton X-100, 5 mM $MgCl_2$, and 10 mM Hepes) containing 0.2 mM PMSF. The homogenates were then centrifuged at 4°C and supernatants were dialyzed against 50 mM Tris-HCl buffer, pH 6.8. Protein samples were separated by SDS-PAGE and transferred onto nitrocellulose membranes. Western blotting using anti-mouse CRISP1 made in goat (R&D Systems) or monoclonal anti-tubulin made in mouse were performed as previously described (Maldera et al., 2011).

Indirect immunofluorescence

COC recovered from *Crisp1*$^{+/-}$ and *Crisp1*$^{-/-}$ animals were fixed with 2% paraformaldehyde and permeabilized with 0.1% Triton X-100 after fixation. COC were then incubated in 5% normal goat serum in PBS, washed, and exposed to anti-rat CRISP1 made in rabbit (Maldera et al., 2011; 1:100 in 0.4% PBS-BSA), and washed again. Finally, COC were stained with propidium iodine (0.05 µg/ml), mounted, and observed in a D-Eclipse C1 (E800; Nikon) laser scanning confocal microscope using a plan Apochromat 40× NA 0.95 objective lenses at 22°C. Acquisition software used was EZ-C1 3.7.

In vitro sperm capacitation

Mouse sperm were recovered from an incision in the cauda epididymidis using 300 µl of capacitation medium (Fraser and Drury, 1975) supplemented with 0.3% of BSA under paraffin oil. After swim-out, sperm were diluted to a final concentration of 0.1–10^7 cells/ml and sperm suspensions were incubated for 90 min at 37°C with 5% CO_2 under paraffin oil.

In vitro fertilization assays

Female mice were superovulated by injection (i.p.) of equine chorionic gonadotropin (5 UI; Syntex), followed by the administration (i.p.) of human chorionic gonadotropin (5UI) 48 h later. COC were collected from oviducts 12–13 h after human chorionic gonadotropin administration and inseminated in vitro with capacitated sperm (final concentration 0.5–2 × 10^5 sperm/ml). After coincubation for 3 h at 37°C with 5% CO_2, COC were washed, fixed, and stained with 1 µg/ml Hoechst 33342 and evaluated under an Optiphot microscope (Nikon) using a plan 20× NA 0.50 objective lenses at 22°C. Eggs were considered fertilized if at least one decondensing sperm nucleus was observed in the cytoplasm.

Cumulus penetration assay

Capacitated mouse sperm were incubated for 15 min in medium containing 0.01 µg/µl Hoechst 33342, and then washed with capacitating medium. COC were inseminated (final concentration 0.3 × 10^5 sperm/ml), and after 15 min were washed, fixed, and mounted on slides. The number of sperm present within the cumulus was determined under an Optiphot microscope equipped with epifluorescence using plan 20× NA 0.50 objective lenses at 22°C. Images were captured with a 3CCD camera (dc330E; DAGE-MTI). The acquisition software used was IPlab (version 3.0). When green/red sperm were used, COC were inseminated, mounted without fixation, and observed.

Cumulus dispersion assay

Crisp1$^{+/-}$ and *Crisp1*$^{-/-}$ COC were incubated at different times in 100 µl of medium alone or mixed with 0.3 mg/ml hyaluronidase (type IV; Sigma-Aldrich) at 37°C in an atmosphere of 5% CO_2 in air, and then observed under a stereoscopic microscope (SMZ800; Nikon). The cumulus dispersion status was classified from 0 to 4, 4 being the dispersion observed in intact COC and 0 in denudated eggs. Intermediate values were assigned for intermediate status.

AR assessment

Epididymal sperm were incubated under capacitating conditions in the presence or not of 10 µM CRISP1 and 15 µM progesterone. After capacitation, sperm were processed for Coomassie assessment of AR as described previously (Visconti et al., 1999) with slight modifications. After fixation with 1 vol of 8% paraformaldehyde in PBS (1 h at 4°C), sperm were washed with 0.1 M ammonium acetate, pH 9, mounted on slides, and air dried. Slides were washed by successive immersions in water, methanol, and water (5 min each) and were then incubated in 0.22% Coomassie brilliant blue G250 solution (50% methanol and 10% acetic acid). After staining, slides were thoroughly washed with distilled water, mounted, and immediately observed to avoid diffusion of the stain. Sperm were scored as acrosome intact when a bright blue staining was observed on the dorsal region of the acrosome or as acrosome reacted when staining was patchy or absent.

CRISP1 purification and treatment

Native rat CRISP1 was obtained as previously described (Garberi et al., 1979, 1982) with a purity of 95% according to silver staining. The components of CRISP1 preparation were analyzed by mass spectrometry. In brief, after treatment with DTT and 4-vinylpyridine to alkylate cysteines, CRISP1 preparation was subjected to C8 RP-HPLC. The eluted protein was digested with trypsin and the resulting peptides were purified by C18 RP-HPLC and analyzed with an ESI-ion trap LCQ-Duo mass spectrometer (Thermo Fisher Scientific). Analysis of the data using the search algorithm Mascot and Sequest revealed that all peptides within the sample corresponded to rat CRISP1 (which exhibits 82% homology with mouse CRISP1). Heat-denatured CRISP1 was obtained by hot-shocking (75°C for 10 min) of purified CRISP1, and DTT-treated CRISP1 as well as recombinant CRISP1 were obtained as described previously (Ellerman et al., 2002).

Sperm orientation and pattern of movement

The assays were performed in a modified Zigmond chamber consisting of two wells separated by a 2-mm partition wall (Fabro et al., 2002). One of the wells (W1) was filled with capacitated mouse sperm and the other one (W2) with medium either alone (control) or with attractants. Then, a 1D attractant concentration gradient was formed across the bridge in the partition wall. 15 min after sealing the chamber, sperm movement was recorded at 30 frames/s in the bridge with a Coolpix L20 camera (Nikon) in an Eclipse TS100 microscope (Nikon) using LWD 20×/0.40 Ph1 ADL ∞/1.2 WD 3.0 objective lenses. Sperm tracks were then analyzed with the ImageJ software (version 1.38; National Institutes of Health) and the MtrackJ plugin. The percentage of "oriented sperm" was calculated for 150 analyzed tracks per treatment with the SpermTrack software (version 4.0, Universidad Nacional de Córdoba). For each sperm track, orientation toward W2 was calculated as a ratio between the distances traveled over the X and Y axes ($\Delta X/|\Delta Y|$). When the value of the ratio was >1, the spermatozoon was considered oriented to W2. A CRISP1 dose–response curve (ranging from 1 pM to 10 µM) was performed. Medium alone was used as a negative control and 100 pM progesterone or COC-conditioned medium (COC from five oviducts in 100 µl, overnight at 37°C) was used as a positive control. The pattern of movement was evaluated by means of the fractal dimension (FD; Mortimer et al., 1996). As FD values were analyzed at 30 Hz, the motility pattern of spermatozoa was classified as linear (FD < 1.3), transitional (1.3 < FD < 1.8), or hyperactivated (FD > 1.8; Fabro et al., 2002).

CASA

Sperm aliquots were placed in a prewarmed 20-µm chamber (Leja Slide; Spectrum Technologies) and examined using the Integrated Semen Analysis System version 1.2 (Proiser Projectes i Serveis R+D) at 37°C. For each sample, a minimum of 200 cells distributed in at least 20 different microscopy fields were scored (30 frames acquired at 60 Hz for each measurement). The following parameters were measured: mean path velocity (VAP, µm/s), curvilinear velocity (VCL, µm/s), straight line velocity (VSL, µm/s), linearity (LIN, %), amplitude of lateral head displacement (ALH, µm), and straightness (STR, %). Sperm were considered hyperactivated when presenting VCL ≥ 245, LIN < 38.5%, and ALH ≥ 4.7. These custom cutoffs were calculated according to Bray et al. (2005).

Sperm preparation for electrophysiology

Testicular sperm were obtained from CD-1 mouse testes by mechanical separation of seminiferous tubules (Martínez-López et al., 2009) and suspended with dissociation solution (HS) containing 135 mM NaCl, 5 mM KCl, 2 mM $CaCl_2$, 1 mM $MgSO_4$, 20 mM Hepes, 5 mM glucose, 10 mM lactic acid, and 1 mM piruvic acid, pH 7.4. Epididymal sperm were suspended in Whitten´s medium. Testicular as well as epididymal sperm were stored at 4°C until assayed and, at the desired time, ∼300-µl aliquots of the cell suspension were dispensed into a recording chamber (1 ml total volume) and subjected to electrophysiological recording.

Electrophysiology

Whole-cell macroscopic currents were obtained by patch clamping the sperm cytoplasmic droplet in testicular and epididymal sperm and were analyzed as reported previously (Ren and Xia, 2010; Kirichok and Lishko, 2011; Martínez-López et al., 2011). All recordings were performed using patch-clamp amplifiers (Axopatch 200 and 200B; Molecular Devices) at room temperature (22°C). Pulse protocols, data capture, and data analysis were performed using pCLAMP 9 software (Molecular Devices), Origin 7.5 (Microcal Software), and Sigma Plot 10 (SYSTAT Software). Current records, unless indicated otherwise, were acquired at 20–100 kHz and filtered at 5–10 kHz (internal four-pole Bessel filter) using a computer attached to a DigiData 1200 and 1300A, respectively (Molecular Devices). Patch pipettes were pulled from borosilicate glass (Kimble Queretaro) and had a final resistance between 5–8 MΩ. To study the cold temperature-sensitive TRPM8 currents, a Bipolar Temperature Controller (TC-202A; Warner Instruments) was used. Initial experiments were performed with an extracellular solution containing 118 mM Na-$MetSO_4$, 8 mM NaCl, 2.5 mM $CaCl_2$, 2 mM KSO_4, 1 mM $MgCl_2$, 10 mM Hepes (pH was adjusted to 7.4 with NaOH). The intracellular solution contained 122 mM K-$MetSO_4$, 8 mM KCl, 20 mM KF, 2.5 mM $CaCl_2$, 1 mM $MgCl_2$, 5 mM EGTA, and 10 mM Hepes (pH was adjusted to 7.3 with KOH). Thereafter, because TRPM8 exhibits high selectivity to Cs^+ (Voets et al., 2007), it was used as the principal cation, as it also eliminates K^+ channel contribution. The extracellular solution contained 144 mM Cs-$MetSO_4$, 6 mM CsCl, 2 mM $CaCl_2$, and 10 mM Hepes-Cs, adjusted to pH 7.35 with CsOH. The internal solution contained 130 mM Cs-$MetSO_4$, 8 mM CsCl, 0.9 mM $CaCl_2$, 12 mM EDTA-Cs, and 10 mM Hepes-Cs, adjusted to pH 7.3 with CsOH. The osmolarity of all solutions was adjusted with dextrose. Unless indicated otherwise, currents were recorded in sperm applying a voltage step protocol from to −100 mV to +100 mV in 20-mV increments with a holding potential of 0 mV and lasting the time indicated in the legends. Menthol dissolved in extracellular solution was applied to sperm using a perfusion system (ALA Scientific instruments). CRISP1 and heat-denatured CRISP1 or vehicle controls were applied at the concentrations indicated in the text with a micro-perfusion system (Picospritzer III; General Valve Corp.) close to the cell being recorded. For recording of monovalent CatSper current ($I_{CatSper}$), the pipette divalent-free solution contained 135 mM $CsMeSO_4$, 5 mM CsCl, 10 mM Hepes, 10 mM EGTA, 5 mM Na_2ATP, and 0.5 mM Na_2GTP, pH = 7.3 with CsOH. Bath solution contained 140 mM $CsMeSO_4$, 20 mM Hepes, 1 mM EDTA, pH = 7.4 with CsOH. Seals between the patch pipette and the cytoplasmic droplet in cauda epididymal sperm were formed in HS bath solution. After break-in, the bath solution could be changed for divalent-free solution.

Measurement of membrane potential (E_m)

E_m was measured as previously described (Demarco et al., 2003). Mature sperm from cauda epididymides were collected, diluted in non-capacitating medium, and exposed to 1 µM Dis-C_3-(5). Mitochondrial membrane potential was dissipated with 500 nM carbonyl cyanide m-chlorophenylhydrazone and sperm were incubated for an additional 2 min. Thereafter, 800 µl of the suspension was transferred to a gently stirred cuvette at 37°C, and fluorescence (620/670 nm excitation/emission) was recorded continuously. Calibration was performed as described previously (Demarco et al., 2003) by supplementing with 1 µM valinomycin and with sequential additions of KCl.

Intracellular Ca^{2+} imaging

Epididymal motile mice sperm were collected by swim-up in medium without BSA and $NaHCO_3$ at 37°C for 10 min. Motile cells were incubated with 2 µM Fluo-3 AM and 0.05% pluronic acid for 30 min. Sperm were attached usually by the head on laminin (1 mg/ml) precoated coverslips, allowing their flagella to move continuously. The coverslip was mounted on a chamber (Hardvardmib Apparatus) and placed on the stage of an inverted microscope (Eclipse TE 300; Nikon). Fluorescence illumination was supplied by a Luxeon V Star Lambertian Cyan LED (part no. LXHLLE5C; Lumileds Lighting LLC) attached to a custom-built stroboscopic control box. The LED was mounted into a FlashCube40 assembly with a dichroic mirror (M40-DC400; Rapp Opto Electronic; bandwidths: excitation, 450–490 nm; dichroic mirror 505 nm; and emission, 520–560 nm). The LED output was synchronized to the Exposure Out signal of a iXon 888 CCD camera via the control box to produce a single flash of 2-ms duration per individual exposure. The camera exposure time was set equivalent to the flash duration (2 ms). Images were collected every 500 ms using iQ software (Andor Technology).

Statistical analysis

The percentages of fertilized eggs and ARs were analyzed by the χ^2 test. The number of sperm that penetrated the COC, the percentages of different motility patterns, the membrane potential results, intracellular Ca^{2+} concentration, and the percentages of hyperactivation were analyzed by Student's *t* test. Sperm orientation and cumulus dispersion assays were analyzed using one-way analysis of variance and Tukey's multiple comparison post-test. Results were considered significantly different at $P < 0.05$.

Online supplemental material

Fig. S1 shows the effect of CRISP1 on cumulus integrity. Fig. S2 shows the effect of CRISP1 on the occurrence of spontaneous or progesterone-induced AR. Fig. S3 shows the trajectories observed for mouse sperm in a modified Zigmond chamber. Fig. S4 shows cold-activated TRPM8 currents in testicular and epididymal sperm. Fig. S5 shows the effect of CRISP1 on menthol-induced increase in intracellular Ca^{2+}. Table S1 shows the effect of CRISP1 on sperm motility. Online supplemental material is available at http://www.jcb.org/cgi/content/full/jcb.201412041/DC1.

Acknowledgments

The authors would like to thank Diego Calb, Ludmila Curci, Guillermo Carvajal, Julieta Maldera, and Esteban Tubert for technical assistance; Daniel Lombardo and Pablo Torres for CASA determinations; Andrés Marin Brito and Manuela Besson for designing the sperm trajectory graphs; and J. Michael Bedford for critical review of the manuscript.

This study was supported by a grant from World Health Organization-Resource Maintenance Grant (H9/TSA/037), the National Research Council of Argentina (PIP 2009-290), and the National Agency for Scientific and Technological Promotion (PICT 2011 No. 2023) to P.S. Cuasnicú and by Consejo Nacional de Ciencia y Tecnología, México (128566), Programa de Apoyo a Proyectos de Investigación e Innovación Tecnológica/Universidad Nacional Autónoma de México (IN202312), and the National Institutes of Health (R01HD038082-07A1 to P. Visconti).

The authors declare no competing financial interests.

Submitted: 9 December 2014
Accepted: 20 August 2015

References

Alasmari, W., S. Costello, J. Correia, S.K. Oxenham, J. Morris, L. Fernandes, J. Ramalho-Santos, J. Kirkman-Brown, F. Michelangeli, S. Publicover, and C.L. Barratt. 2013. Ca^{2+} signals generated by CatSper and Ca^{2+} stores regulate different behaviors in human sperm. *J. Biol. Chem.* 288:6248–6258. http://dx.doi.org/10.1074/jbc.M112.439356

Armon, L., and M. Eisenbach. 2011. Behavioral mechanism during human sperm chemotaxis: involvement of hyperactivation. *PLoS ONE.* 6:e28359. http://dx.doi.org/10.1371/journal.pone.0028359

Boryshpolets, S., S. Pérez-Cerezales, and M. Eisenbach. 2015. Behavioral mechanism of human sperm in thermotaxis: a role for hyperactivation. *Hum. Reprod.* 30:884–892. http://dx.doi.org/10.1093/humrep/dev002

Bray, C., J.H. Son, P. Kumar, and S. Meizel. 2005. Mice deficient in CHRNA7, a subunit of the nicotinic acetylcholine receptor, produce sperm with impaired motility. *Biol. Reprod.* 73:807–814. http://dx.doi.org/10.1095/biolreprod.105.042184

Brenker, C., N. Goodwin, I. Weyand, N.D. Kashikar, M. Naruse, M. Krähling, A. Müller, U.B. Kaupp, and T. Strünker. 2012. The CatSper channel: a polymodal chemosensor in human sperm. *EMBO J.* 31:1654–1665. http://dx.doi.org/10.1038/emboj.2012.30

Brown, R.L., T.L. Haley, K.A. West, and J.W. Crabb. 1999. Pseudechetoxin: a peptide blocker of cyclic nucleotide-gated ion channels. *Proc. Natl. Acad. Sci. USA.* 96:754–759. http://dx.doi.org/10.1073/pnas.96.2.754

Burnett, L.A., S. Boyles, C. Spencer, A.L. Bieber, and D.E. Chandler. 2008. *Xenopus tropicalis* allurin: expression, purification, and characterization of a sperm chemoattractant that exhibits cross-species activity. *Dev. Biol.* 316:408–416. http://dx.doi.org/10.1016/j.ydbio.2008.01.046

Burnett, L.A., D.M. Anderson, A. Rawls, A.L. Bieber, and D.E. Chandler. 2011a. Mouse sperm exhibit chemotaxis to allurin, a truncated member of the cysteine-rich secretory protein family. *Dev. Biol.* 360:318–328. http://dx.doi.org/10.1016/j.ydbio.2011.09.028

Burnett, L.A., H. Sugiyama, A.L. Bieber, and D.E. Chandler. 2011b. Egg jelly proteins stimulate directed motility in *Xenopus laevis* sperm. *Mol. Reprod. Dev.* 78:450–462. http://dx.doi.org/10.1002/mrd.21325

Burnett, L.A., C.A. Washburn, H. Sugiyama, X. Xiang, J.H. Olson, B. Al-Anzi, A.L. Bieber, and D.E. Chandler. 2012. Allurin, an amphibian sperm chemoattractant having implications for mammalian sperm physiology. *Int. Rev. Cell. Mol. Biol.* 295:1–61. http://dx.doi.org/10.1016/B978-0-12-394306-4.00007-1

Busso, D., D.J. Cohen, J.A. Maldera, A. Dematteis, and P.S. Cuasnicu. 2007. A novel function for CRISP1 in rodent fertilization: involvement in sperm-zona pellucida interaction. *Biol. Reprod.* 77:848–854. http://dx.doi.org/10.1095/biolreprod.107.061788

Cameo, M.S., and J.A. Blaquier. 1976. Androgen-controlled specific proteins in rat epididymis. *J. Endocrinol.* 69:47–55. http://dx.doi.org/10.1677/joe.0.0690047

Carlson, A.E., L.A. Burnett, D. del Camino, T.A. Quill, B. Hille, J.A. Chong, M.M. Moran, and D.F. Babcock. 2009. Pharmacological targeting of native CatSper channels reveals a required role in maintenance of sperm hyperactivation. *PLoS ONE.* 4:e6844. http://dx.doi.org/10.1371/journal.pone.0006844

Chang, H., and S.S. Suarez. 2010. Rethinking the relationship between hyperactivation and chemotaxis in mammalian sperm. *Biol. Reprod.* 83:507–513. http://dx.doi.org/10.1095/biolreprod.109.083113

Chang, H., and S.S. Suarez. 2011. Two distinct Ca^{2+} signaling pathways modulate sperm flagellar beating patterns in mice. *Biol. Reprod.* 85:296–305. http://dx.doi.org/10.1095/biolreprod.110.089789

Cohen, D.J., D.A. Ellerman, and P.S. Cuasnicú. 2000a. Mammalian sperm-egg fusion: evidence that epididymal protein DE plays a role in mouse gamete fusion. *Biol. Reprod.* 63:462–468. http://dx.doi.org/10.1095/biolreprod63.2.462

Cohen, D.J., L. Rochwerger, D.A. Ellerman, M.M. Morgenfeld, D. Busso, and P.S. Cuasnicú. 2000b. Relationship between the association of rat epididymal protein "DE" with spermatozoa and the behavior and function of the protein. *Mol. Reprod. Dev.* 56:180–188. http://dx.doi.org/10.1002/(SICI)1098-2795(200006)56:2<180::AID-MRD9>3.0.CO;2-4

Cohen, D.J., D.A. Ellerman, D. Busso, M.M. Morgenfeld, A.D. Piazza, M. Hayashi, E.T. Young, M. Kasahara, and P.S. Cuasnicu. 2001. Evidence that human epididymal protein ARP plays a role in gamete fusion through complementary sites on the surface of the human egg. *Biol. Reprod.* 65:1000–1005. http://dx.doi.org/10.1095/biolreprod65.4.1000

Cohen, D.J., J.A. Maldera, G. Vasen, J.I. Ernesto, M.W. Muñoz, M.A. Battistone, and P.S. Cuasnicú. 2011. Epididymal protein CRISP1 plays different roles during the fertilization process. *J. Androl.* 32:672–678. http://dx.doi.org/10.2164/jandrol.110.012922

Da Ros, V.G., J.A. Maldera, W.D. Willis, D.J. Cohen, E.H. Goulding, D.M. Gelman, M. Rubinstein, E.M. Eddy, and P.S. Cuasnicu. 2008. Impaired sperm fertilizing ability in mice lacking Cysteine-RIch Secretory Protein 1 (CRISP1). *Dev. Biol.* 320:12–18. http://dx.doi.org/10.1016/j.ydbio.2008.03.015

Darszon, A., T. Nishigaki, C. Beltran, and C.L. Treviño. 2011. Calcium channels in the development, maturation, and function of spermatozoa. *Physiol. Rev.* 91:1305–1355. http://dx.doi.org/10.1152/physrev.00028.2010

Demarco, I.A., F. Espinosa, J. Edwards, J. Sosnik, J.L. De La Vega-Beltran, J.W. Hockensmith, G.S. Kopf, A. Darszon, and P.E. Visconti. 2003. Involvement of a Na^+/HCO_3^- cotransporter in mouse sperm capacitation. *J. Biol. Chem.* 278:7001–7009. http://dx.doi.org/10.1074/jbc.M206284200

Ellerman, D.A., V.G. Da Ros, D.J. Cohen, D. Busso, M.M. Morgenfeld, and P.S. Cuasnicú. 2002. Expression and structure-function analysis of de, a sperm cysteine-rich secretory protein that mediates gamete fusion. *Biol. Reprod.* 67:1225–1231. http://dx.doi.org/10.1095/biolreprod67.4.1225

Espinosa, F., and A. Darszon. 1995. Mouse sperm membrane potential: changes induced by Ca^{2+}. *FEBS Lett.* 372:119–125. http://dx.doi.org/10.1016/0014-5793(95)00962-9

Fabro, G., R.A. Rovasio, S. Civalero, A. Frenkel, S.R. Caplan, M. Eisenbach, and L.C. Giojalas. 2002. Chemotaxis of capacitated rabbit spermatozoa to follicular fluid revealed by a novel directionality-based assay. *Biol. Reprod.* 67:1565–1571. http://dx.doi.org/10.1095/biolreprod.102.006395

Fraser, L.R., and L.M. Drury. 1975. The relationship between sperm concentration and fertilization *in vitro* of mouse eggs. *Biol. Reprod.* 13:513–518. http://dx.doi.org/10.1095/biolreprod13.5.513

Garberi, J.C., A.C. Kohane, M.S. Cameo, and J.A. Blaquier. 1979. Isolation and characterization of specific rat epididymal proteins. *Mol. Cell. Endocrinol.* 13:73–82. http://dx.doi.org/10.1016/0303-7207(79)90077-7

Garberi, J.C., J.D. Fontana, and J.A. Blaquier. 1982. Carbohydrate composition of specific rat epididymal protein. *Int. J. Androl.* 5:619–626. http://dx.doi.org/10.1111/j.1365-2605.1982.tb00296.x

Gibbs, G.M., M.J. Scanlon, J. Swarbrick, S. Curtis, E. Gallant, A.F. Dulhunty, and M.K. O'Bryan. 2006. The cysteine-rich secretory protein domain of Tpx-1 is related to ion channel toxins and regulates ryanodine receptor Ca^{2+} signaling. *J. Biol. Chem.* 281:4156–4163. http://dx.doi.org/10.1074/jbc.M506849200

Gibbs, G.M., K. Roelants, and M.K. O'Bryan. 2008. The CAP superfamily: cysteine-rich secretory proteins, antigen 5, and pathogenesis-related 1 proteins—roles in reproduction, cancer, and immune defense. *Endocr. Rev.* 29:865–897. http://dx.doi.org/10.1210/er.2008-0032

Gibbs, G.M., G. Orta, T. Reddy, A.J. Koppers, P. Martínez-López, J.L. de la Vega-Beltràn, J.C. Lo, N. Veldhuis, D. Jamsai, P. McIntyre, et al. 2011. Cysteine-rich secretory protein 4 is an inhibitor of transient receptor potential M8 with a role in establishing sperm function. *Proc. Natl. Acad. Sci. USA.* 108:7034–7039. http://dx.doi.org/10.1073/pnas.1015935108

Grimm, C., R. Kraft, S. Sauerbruch, G. Schultz, and C. Harteneck. 2003. Molecular and functional characterization of the melastatin-related cation channel TRPM3. *J. Biol. Chem.* 278:21493–21501. http://dx.doi.org/10.1074/jbc.M300945200

Guerrero, A., T. Nishigaki, J. Carneiro, C.D. Yoshiro Tatsu, Wood, and A. Darszon. 2010. Tuning sperm chemotaxis by calcium burst timing. *Dev. Biol.* 344:52–65. http://dx.doi.org/10.1016/j.ydbio.2010.04.013

Guidobaldi, H.A., M.E. Teves, D.R. Uñates, A. Anastasía, and L.C. Giojalas. 2008. Progesterone from the cumulus cells is the sperm chemoattractant secreted by the rabbit oocyte cumulus complex. *PLoS ONE.* 3:e3040. http://dx.doi.org/10.1371/journal.pone.0003040

Guidobaldi, H.A., M.E. Teves, D.R. Uñates, and L.C. Giojalas. 2012. Sperm transport and retention at the fertilization site is orchestrated by a chemical guidance and oviduct movement. *Reproduction.* 143:587–596. http://dx.doi.org/10.1530/REP-11-0478

Guo, M., M. Teng, L. Niu, Q. Liu, Q. Huang, and Q. Hao. 2005. Crystal structure of the cysteine-rich secretory protein stecrisp reveals that the cysteine-rich domain has a K^+ channel inhibitor-like fold. *J. Biol. Chem.* 280:12405–12412. http://dx.doi.org/10.1074/jbc.M413566200

Hasuwa, H., Y. Muro, M. Ikawa, N. Kato, Y. Tsujimoto, and M. Okabe. 2010. Transgenic mouse sperm that have green acrosome and red mitochondria allow visualization of sperm and their acrosome reaction in vivo. *Exp. Anim.* 59:105–107. http://dx.doi.org/10.1538/expanim.59.105

Hunter, R.H., and H. Rodriguez-Martinez. 2004. Capacitation of mammalian spermatozoa in vivo, with a specific focus on events in the fallopian tubes. *Mol. Reprod. Dev.* 67:243–250. http://dx.doi.org/10.1002/mrd.10390

Kirichok, Y., and P.V. Lishko. 2011. Rediscovering sperm ion channels with the patch-clamp technique. *Mol. Hum. Reprod.* 17:478–499. http://dx.doi.org/10.1093/molehr/gar044

Kirichok, Y., B. Navarro, and D.E. Clapham. 2006. Whole-cell patch-clamp measurements of spermatozoa reveal an alkaline-activated Ca^{2+} channel. *Nature.* 439:737–740. http://dx.doi.org/10.1038/nature04417

Kohane, A.C., F.M. González Echeverría, L. Piñeiro, and J.A. Blaquier. 1980. Interaction of proteins of epididymal origin with spermatozoa. *Biol. Reprod.* 23:737–742. http://dx.doi.org/10.1095/biolreprod23.4.737

Lishko, P.V., and Y. Kirichok. 2010. The role of Hv1 and CatSper channels in sperm activation. *J. Physiol.* 588:4667–4672. http://dx.doi.org/10.1113/jphysiol.2010.194142

Lishko, P.V., I.L. Botchkina, and Y. Kirichok. 2011. Progesterone activates the principal Ca^{2+} channel of human sperm. *Nature.* 471:387–391. http://dx.doi.org/10.1038/nature09767

Lishko, P.V., Y. Kirichok, D. Ren, B. Navarro, J.J. Chung, and D.E. Clapham. 2012. The control of male fertility by spermatozoan ion channels. *Annu. Rev. Physiol.* 74:453–475. http://dx.doi.org/10.1146/annurev-physiol-020911-153258

Maldera, J.A., G. Vasen, J.I. Ernesto, M. Weigel-Muñoz, D.J. Cohen, and P.S. Cuasnicu. 2011. Evidence for the involvement of zinc in the association of CRISP1 with rat sperm during epididymal maturation. *Biol. Reprod.* 85:503–510. http://dx.doi.org/10.1095/biolreprod.111.091439

Maldera, J.A., M. Weigel Muñoz, M. Chirinos, D. Busso, F. G E Raffo, M.A. Battistone, J.A. Blaquier, F. Larrea, and P.S. Cuasnicu. 2014. Human fertilization: epididymal hCRISP1 mediates sperm-zona pellucida binding through its interaction with ZP3. *Mol. Hum. Reprod.* 20:341–349. http://dx.doi.org/10.1093/molehr/gat092

Mälkiä, A., R. Madrid, V. Meseguer, E. de la Peña, M. Valero, C. Belmonte, and F. Viana. 2007. Bidirectional shifts of TRPM8 channel gating by temperature and chemical agents modulate the cold sensitivity of mammalian thermoreceptors. *J. Physiol.* 581:155–174. http://dx.doi.org/10.1113/jphysiol.2006.123059

Martínez-López, P., C.M. Santi, C.L. Treviño, A.Y. Ocampo-Gutiérrez, J.J. Acevedo, A. Alisio, L.B. Salkoff, and A. Darszon. 2009. Mouse sperm K^+ currents stimulated by pH and cAMP possibly coded by Slo3 channels. *Biochem. Biophys. Res. Commun.* 381:204–209. http://dx.doi.org/10.1016/j.bbrc.2009.02.008

Martínez-López, P., C.L. Treviño, J.L. de la Vega-Beltrán, G. De Blas, E. Monroy, C. Beltrán, G. Orta, G.M. Gibbs, M.K. O'Bryan, and A. Darszon. 2011. TRPM8 in mouse sperm detects temperature changes and may influence the acrosome reaction. *J. Cell. Physiol.* 226:1620–1631. http://dx.doi.org/10.1002/jcp.22493

Miki, K., and D.E. Clapham. 2013. Rheotaxis guides mammalian sperm. *Curr. Biol.* 23:443–452. http://dx.doi.org/10.1016/j.cub.2013.02.007

Morrissette, J., J. Krätzschmar, B. Haendler, R. el-Hayek, J. Mochca-Morales, B.M. Martin, J.R. Patel, R.L. Moss, W.D. Schleuning, R. Coronado, and L.D. Possani. 1995. Primary structure and properties of helothermine, a peptide toxin that blocks ryanodine receptors. *Biophys. J.* 68:2280–2288. http://dx.doi.org/10.1016/S0006-3495(95)80410-8

Mortimer, S.T., M.A. Swan, and D. Mortimer. 1996. Fractal analysis of capacitating human spermatozoa. *Hum. Reprod.* 11:1049–1054. http://dx.doi.org/10.1093/oxfordjournals.humrep.a019295

Olson, J.H., X. Xiang, T. Ziegert, A. Kittelson, A. Rawls, A.L. Bieber, and D.E. Chandler. 2001. Allurin, a 21-kDa sperm chemoattractant from *Xenopus* egg jelly, is related to mammalian sperm-binding proteins. *Proc. Natl. Acad. Sci. USA.* 98:11205–11210. http://dx.doi.org/10.1073/pnas.211316798

Publicover, S.J., L.C. Giojalas, M.E. Teves, G.S. de Oliveira, A.A. Garcia, C.L. Barratt, and C.V. Harper. 2008. Ca^{2+} signalling in the control of motility and guidance in mammalian sperm. *Front. Biosci.* 13:5623–5637. http://dx.doi.org/10.2741/3105

Reddy, T., G.M. Gibbs, D.J. Merriner, J.B. Kerr, and M.K. O'Bryan. 2008. Cysteine-rich secretory proteins are not exclusively expressed in the male reproductive tract. *Dev. Dyn.* 237:3313–3323. http://dx.doi.org/10.1002/dvdy.21738

Ren, D., and J. Xia. 2010. Calcium signaling through CatSper channels in mammalian fertilization. *Physiology (Bethesda).* 25:165–175. http://dx.doi.org/10.1152/physiol.00049.2009

Ren, D., B. Navarro, G. Perez, A.C. Jackson, S. Hsu, Q. Shi, J.L. Tilly, and D.E. Clapham. 2001. A sperm ion channel required for sperm motility and male fertility. *Nature.* 413:603–609. http://dx.doi.org/10.1038/35098027

Roberts, K.P., J.A. Wamstad, K.M. Ensrud, and D.W. Hamilton. 2003. Inhibition of capacitation-associated tyrosine phosphorylation signaling in rat sperm by epididymal protein Crisp-1. *Biol. Reprod.* 69:572–581. http://dx.doi.org/10.1095/biolreprod.102.013771

Rochwerger, L., and P.S. Cuasnicu. 1992. Redistribution of a rat sperm epididymal glycoprotein after in vitro and in vivo capacitation. *Mol. Reprod. Dev.* 31:34–41. http://dx.doi.org/10.1002/mrd.1080310107

Rochwerger, L., D.J. Cohen, and P.S. Cuasnicú. 1992. Mammalian sperm-egg fusion: the rat egg has complementary sites for a sperm protein that mediates gamete fusion. *Dev. Biol.* 153:83–90. http://dx.doi.org/10.1016/0012-1606(92)90093-V

Smith, J.F., O. Syritsyna, M. Fellous, C. Serres, N. Mannowetz, Y. Kirichok, and P.V. Lishko. 2013. Disruption of the principal, progesterone-activated sperm Ca^{2+} channel in a CatSper2-deficient infertile patient. *Proc. Natl. Acad. Sci. USA.* 110:6823–6828. http://dx.doi.org/10.1073/pnas.1216588110

Strünker, T., N. Goodwin, C. Brenker, N.D. Kashikar, I. Weyand, R. Seifert, and U.B. Kaupp. 2011. The CatSper channel mediates progesterone-induced Ca^{2+} influx in human sperm. *Nature.* 471:382–386. http://dx.doi.org/10.1038/nature09769

Suárez, S.S., and R.A. Osman. 1987. Initiation of hyperactivated flagellar bending in mouse sperm within the female reproductive tract. *Biol. Reprod.* 36:1191–1198. http://dx.doi.org/10.1095/biolreprod36.5.1191

Sun, F., A. Bahat, A. Gakamsky, E. Girsh, N. Katz, L.C. Giojalas, I. Tur-Kaspa, and M. Eisenbach. 2005. Human sperm chemotaxis: both the oocyte and its surrounding cumulus cells secrete sperm chemoattractants. *Hum. Reprod.* 20:761–767. http://dx.doi.org/10.1093/humrep/deh657

Suzuki, N., Y. Yamazaki, R.L. Brown, Z. Fujimoto, T. Morita, and H. Mizuno. 2008. Structures of pseudechetoxin and pseudecin, two snake-venom cysteine-rich secretory proteins that target cyclic nucleotide-gated ion channels: implications for movement of the C-terminal cysteine-rich domain. *Acta Crystallogr. D Biol. Crystallogr.* 64:1034–1042. http://dx.doi.org/10.1107/S0907444908023512

Tesarík, J., C. Mendoza Oltras, and J. Testart. 1990. Effect of the human cumulus oophorus on movement characteristics of human capacitated spermatozoa. *J. Reprod. Fertil.* 88:665–675. http://dx.doi.org/10.1530/jrf.0.0880665

Teves, M.E., F. Barbano, H.A. Guidobaldi, R. Sanchez, W. Miska, and L.C. Giojalas. 2006. Progesterone at the picomolar range is a chemoattractant for mammalian spermatozoa. *Fertil. Steril.* 86:745–749. http://dx.doi.org/10.1016/j.fertnstert.2006.02.080

Torres-Flores, V., G. Picazo-Juárez, Y. Hernández-Rueda, A. Darszon, and M.T. González-Martínez. 2011. Sodium influx induced by external calcium chelation decreases human sperm motility. *Hum. Reprod.* 26:2626–2635. http://dx.doi.org/10.1093/humrep/der237

Visconti, P.E., X. Ning, M.W. Fornés, J.G. Alvarez, P. Stein, S.A. Connors, and G.S. Kopf. 1999. Cholesterol efflux-mediated signal transduction in mammalian sperm: cholesterol release signals an increase in protein tyrosine phosphorylation during mouse sperm capacitation. *Dev. Biol.* 214:429–443. http://dx.doi.org/10.1006/dbio.1999.9428

Voets, T., G. Owsianik, A. Janssens, K. Talavera, and B. Nilius. 2007. TRPM8 voltage sensor mutants reveal a mechanism for integrating thermal and chemical stimuli. *Nat. Chem. Biol.* 3:174–182. http://dx.doi.org/10.1038/nchembio862

Wang, F., H. Li, M.N. Liu, H. Song, H.M. Han, Q.L. Wang, C.C. Yin, Y.C. Zhou, Z. Qi, Y.Y. Shu, et al. 2006. Structural and functional analysis of natrin, a venom protein that targets various ion channels. *Biochem. Biophys. Res. Commun.* 351:443–448. http://dx.doi.org/10.1016/j.bbrc.2006.10.067

Xiang, X., A. Kittelson, J. Olson, A. Bieber, and D. Chandler. 2005. Allurin, a 21 kD sperm chemoattractant, is rapidly released from the outermost jelly layer of the *Xenopus* egg by diffusion and medium convection. *Mol. Reprod. Dev.* 70:344–360. http://dx.doi.org/10.1002/mrd.20201

Yamazaki, Y., R.L. Brown, and T. Morita. 2002. Purification and cloning of toxins from elapid venoms that target cyclic nucleotide-gated ion channels. *Biochemistry.* 41:11331–11337. http://dx.doi.org/10.1021/bi026132h

Yanagimachi, R. 1994. Mammalian fertilization. *In* The Physiology of Reproduction. E. Knobil, and J.D. Neill, editors. Raven Press, New York. 189–317.

Yoshida, M., and K. Yoshida. 2011. Sperm chemotaxis and regulation of flagellar movement by Ca^{2+}. *Mol. Hum. Reprod.* 17:457–465. http://dx.doi.org/10.1093/molehr/gar041

Zeng, X.H., B. Navarro, X.M. Xia, D.E. Clapham, and C.J. Lingle. 2013. Simultaneous knockout of Slo3 and CatSper1 abolishes all alkalization- and voltage-activated current in mouse spermatozoa. *J. Gen. Physiol.* 142:305–313. http://dx.doi.org/10.1085/jgp.201311011

Zhou, Q., Q.L. Wang, X. Meng, Y. Shu, T. Jiang, T. Wagenknecht, C.C. Yin, S.F. Sui, and Z. Liu. 2008. Structural and functional characterization of ryanodine receptor-natrin toxin interaction. *Biophys. J.* 95:4289–4299. http://dx.doi.org/10.1529/biophysj.108.137224